J|A|C|S COMMUNICATIONS

Published on Web 09/16/2009

Postsynthetic Modifications of Iron-Carboxylate Nanoscale Metal−Organic Frameworks for Imaging and Drug Delivery

Kathryn M. L. Taylor-Pashow, Joseph Della Rocca, Zhigang Xie, Sylvie Tran, and Wenbin Lin*

Department of Chemistry, CB#3290, University of North Carolina, Chapel Hill, North Carolina 27599

Received July 23, 2009; E-mail: wlin@unc.edu

Metal−organic frameworks (MOFs) are a class of hybrid materials with infinite tunability that results from the limitless choice of metals and organic bridging ligands.[1] MOFs can also be designed to exhibit unprecedentedly high porosity.[2] Among the tens of thousands of known MOFs, the MIL family built from trivalent metal centers and carboxylate bridging ligands pioneered by Férey and co-workers has particularly attracted a great deal of attention due to their enhanced stability, enormous porosity, and very large pores.[3] For example, MIL-101 (Cr) with the formula $Cr_3F(H_2O)_2O(BDC)_3 \cdot nH_2O$ (where n is ~25) has a Langmuir surface area of up to 5900 m^2/g and contains two types of mesoporous cages with internal free diameters of ~29 and 34 Å.[4] The combination of these features makes the MIL family a unique candidate for storage and controlled release of biologically important molecules. Indeed, Férey and co-workers have elegantly demonstrated the loading of organic drug molecules in the large pores of the bulk phases of MILs via physical absorption.[5] They have shown that MIL-101 (Cr) can adsorb 138 wt % ibuprofen and MIL-53 can adsorb 22 wt % ibuprofen.[5] The release of ibuprofen from the MILs was evaluated using simulated body fluid at 37 °C. It was found that the MIL-101 (Cr) released ibuprofen slowly in several stages, reaching completion after 6 days.[5a] The MIL-53 materials showed an even slower release, reaching completion after 21 days.[5b]

In order for MOFs to be useful as efficient delivery vehicles for drugs and imaging contrast agents, the material composition must be biocompatible and the particle sizes must be carefully controlled to be uniform and below several hundred nanometers.[6] We have recently demonstrated the potential application of nanoscale metal−organic frameworks (NMOFs) in magnetic resonance imaging and anticancer drug delivery.[7] The imaging and drug components in the previous systems were directly incorporated into the NMOFs either as metal-connecting points or as bridging ligands during the NMOF synthesis.[7] Herein we report a new strategy of delivering an imaging contrast agent and an anticancer drug by postsynthetic modifications of a highly porous NMOF. We demonstrated for the first time the synthesis of an iron-carboxylate NMOF of the MIL-101 structure and the loading of an organic fluorophore and an anticancer drug via covalent modifications of the as-synthesized nanoparticles.[8] The potential utility of such a novel nanodelivery system in optical imaging and anticancer therapy was also demonstrated *in vitro*.

Fe(III) NMOF particles with the framework formula of $Fe_3(\mu_3\text{-}O)Cl(H_2O)_2(BDC)_3$ (**1**) were synthesized in modest yields (typically ~20%) by heating a solution of equimolar $FeCl_3$ and terephthalic acid (BDC) in DMF at 150 °C with microwave heating. The particles were isolated by centrifuging and washed with DMF and ethanol to remove any unreacted starting materials. Scanning electron microscopy (SEM) images show that the particles of **1** have an unusual octahedron morphology and an average diameter of ~200 nm (Figure 1a). Powder X-ray diffraction (PXRD) studies indicated that particles of **1** are highly crystalline and of the same structure as the MIL-101 (Cr) (Figure 2).[4] To our knowledge, the Fe(III) analogue of MIL-101 (either bulk phase or nanoparticle form) has not been previously reported. Nitrogen adsorption studies showed that particles of **1** are highly porous with a Langmuir surface area ranging from 3700 to 4535 m^2/g, a value that is slightly lower than that reported for the bulk MIL-101 (Cr). The slightly lower porosity of **1** as compared to the bulk phase of MIL-101 (Cr) is presumably due to structural defects present in the nanosized MIL-101 (Fe).

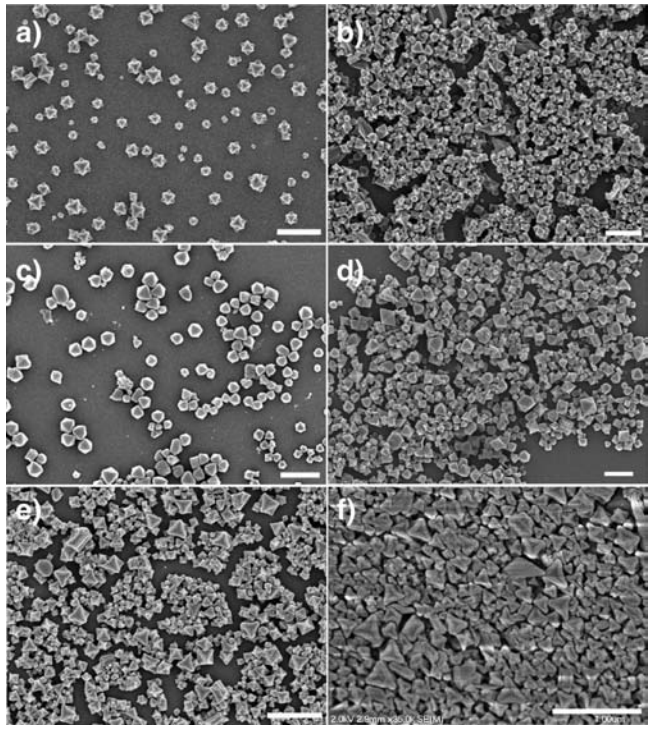

Figure 1. (a) SEM image of $Fe_3(\mu_3\text{-}O)Cl(H_2O)_2(BDC)_3$ nanoparticles (**1**). (b) SEM image of nanoparticles of **1a** with 17.4 mol % NH_2-BDC. (c) SEM of nanoparticles of **1a** loaded with the BODIPY dye (**1b**). (d) SEM image of nanoparticles of **1a** loaded with *c*,*c*,*t*-$[PtCl_2(NH_3)_2(OEt)(O_2CCH_2CH_2CO_2H)]$ (**1c**). (e) SEM image of silica-coated nanoparticles of **1**. (f) SEM image of silica-coated nanoparticles of **1c**. The scale bars represent 1 μm.

In order to allow for postsynthetic modifications of the MIL-101 (Fe) nanoparticles, we attempted to synthesize amino-functionalized particles of **1** (denoted as **1a**) by incorporating 2-aminoterephthalic acid (NH_2-BDC). Interestingly, as shown by PXRD studies, although the particles of **1a** with low NH_2-BDC incorporation (up to 17.5 mol % of NH_2-BDC in the feed) exhibited the same MIL-101 structure as **1** (Figure 2), the particles with higher NH_2-BDC incorporation (greater than 20 mol % of NH_2-BDC in the feed) adopted the MIL-88B structure (denoted as **2**; see

Supporting Information).[9] The amount of NH_2-BDC incorporated into **1a** was quantified by NMR after digesting the particles with Na_4EDTA and methylating the carboxylate groups of BDC and NH_2-BDC. The ratio of NH_2-BDC incorporation was slightly higher than the ratio in the feed in most cases except the sample with 17.5 mol % NH_2-BDC in the feed that had 17.4 mol % NH_2-BDC incorporation. The sizes and morphologies of the **1a** particles are similar to those of **1** regardless of the NH_2-BDC percentage (Figure 1b).[10] The **1a** particles with 17.4 mol % NH_2-BDC were used for all the subsequent studies in this work.

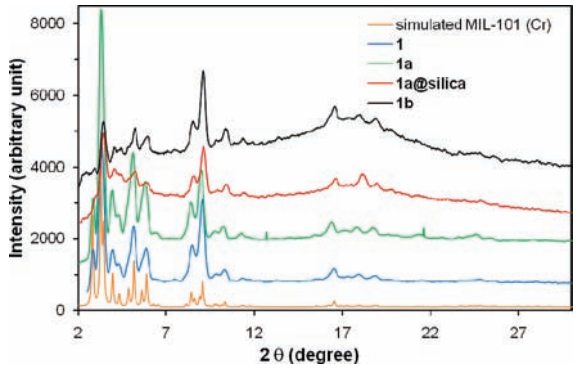

Figure 2. PXRD patterns of MIL-101 (Cr) simulated form the CIF file, MIL-101 (Fe) nanoparticles (**1**), amino-containing nanoparticles (**1a**), silica-coated particles (**1a**@silica), and BODIPY-loaded particles (**1b**).

The presence of amino groups on the particles of **1a** allows for covalent attachment of biologically relevant cargoes through postsynthetic modifications (Scheme 1). Based on our previous work, we expect NMOFs **1** and **1a** to be biodegradable and to provide an interesting nanodelivery vehicle for imaging contrast agents and anticancer drugs by slow release of the cargoes via NMOF degradation. We first loaded a optical imaging contrast agent by treating **1a** particles with 1,3,5,7-tetramethyl-4,4-difluoro-8-bromomethyl-4-bora-3*a*,4*a*-diaza-*s*-indacene (Br-BODIPY) in THF at rt for 2 days. The BODIPY-loaded particles (**1b**) were isolated by centrifuging, and the unreacted dye was removed by washing with THF. The BODIPY loading was determined to be 5.6−11.6 wt % based on the absorbance of the BDC-NH-BODIPY dye (at 498 nm) after digesting the **1b** particles with Na_4EDTA. This

Scheme 1

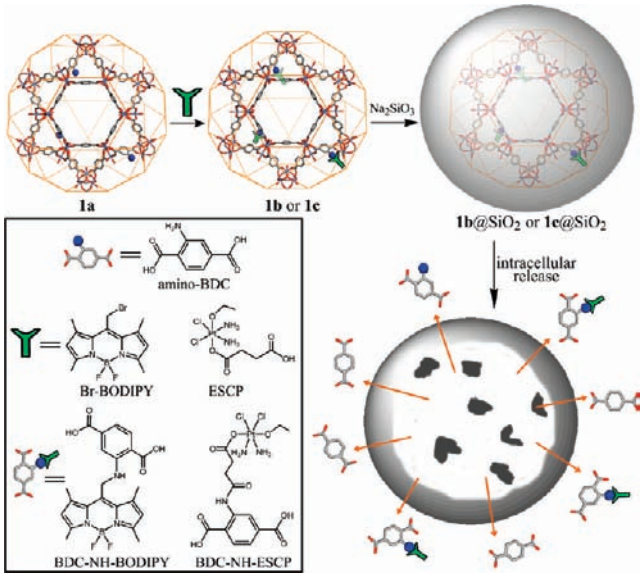

corresponds to an NH_2-BDC to BDC-NH-BODIPY conversion efficiency of 20.9 to 40.3%. Thermogravimetric analysis (TGA) showed an increased weight loss that is consistent with the BODIPY grafting. SEM images show that the sizes and morphologies of the particles **1a** remain essentially unchanged after BODIPY loading (Figure 1c). PXRD studies indicated the particles of **1b** maintain the MIL-101 structure (Figure 2). BODIPY-grafted **1b** is nonemissive due to luminescence quenching by the d−d transitions of the Fe(III) centers.

We also loaded a prodrug of cisplatin into **1a** by postsynthetic modification. The ethoxysuccinato-cisplatin (ESCP) prodrug, *c*,*c*,*t*-$[PtCl_2(NH_3)_2(OEt)(O_2CCH_2CH_2CO_2H)]$, was first activated by 1,1-carbonydiimidazole and then reacted with a dispersion of **1a** in DMF at room temperature. The ESCP-loaded particles **1c** were isolated by centrifuging and washed with DMF and ethanol. SEM imaging showed no change in the particle size or morphology after ESCP loading (Figure 1d), whereas PXRD studies showed that the ESCP-loaded particles (**1c**) retained the MIL-101 structure. The ICP-MS results showed that the Pt/Fe weight ratio for **1c** with 16 mol % NH_2-BDC was 0.208. A Pt/Fe weight ratio of 0.559 would be expected if all the amino groups had been functionalized with the ESCP. 37.3% of all the available NH_2-BDC groups in **1c** were thus functionalized with ESCP. For a sample of **1c** with 17.4 mol % NH_2-BDC, a Pt/Fe weight ratio of 0.244 was obtained, which represents a conversion efficiency of 40.2% of NH_2-BDC to BDC-NH-ESCP. Amino-functionalized MIL-101 (Fe) nanoparticles thus provide an efficient platform for delivering the ESCP prodrug with an overall payload of 12.8 wt %. Particles **1c** with 17.4 mol % NH_2-BDC were used for subsequent experiments.

The covalent grafting of BODIPY and ESCP allowed us to determine the stability of MIL-101 (Fe) nanoparticles in biologically relevant media. As the BODIPY dye is released from the **1b** particles, the solution exhibits a fluorescence signal characteristic of the BDC-NH-BODIPY species. The release of the BODIPY dye from **1b** was determined by measuring the fluorescence spectra of the aliquots at different time points. As shown in Figure 3, the BDC-NH-BODIPY dye is readily released from the **1b** particles with a $t_{1/2}$ of ∼2.5 h in 8 mM PBS buffer at 37 °C. Since the BODIPY dye is covalently attached to the NH_2-BDC via the robust amine linkage, the release of BODIPY must be due to the degradation of the **1b** particles. Consistent with this, the recovered particles lost the diffraction peaks due to the MIL-101 structure, suggesting the formation of the amorphous iron phosphate (Scheme 1). We verified the degradation of MIL-101 (Fe) nanoparticles in PBS buffer by examining the release of BDC-NH-ESCP from the **1c** particles.[11] ICP-MS studies indicated that the BDC-NH-ESCP was steadily released from **1c** with a $t_{1/2}$ of ∼1.2 h in PBS buffer at 37 °C (Figure 3).

Because of the instability of the nanosized MIL-101 (Fe) particles in PBS buffer, we attempted to slow down the cargo release by coating the particles with a thin silica layer. Numerous attempts using a previously established procedure based on base-catalyzed hydrolysis of tetraethoxysilane led to the decomposition of the particles of **1**.[12] The nanosized MIL-101 (Fe) particles readily decompose under basic conditions to presumably form amorphous iron hydroxide (oxide) phases. An alternative procedure using Na_2SiO_3 as the silica source led to successful coating of MIL-101 (Fe) nanoparticles with a uniform layer of silica. SEM imaging showed no discernible change of the morphology upon silica coating (Figure 1e), but energy dispersive X-ray (EDX) analysis showed the presence of silicon (with a Si/Fe molar ratio of 1.4) in the particles of **1**@silica. Consistent with this, TGA analysis indicated a decreased percent weight loss (by ∼26%) in the 200−400 °C

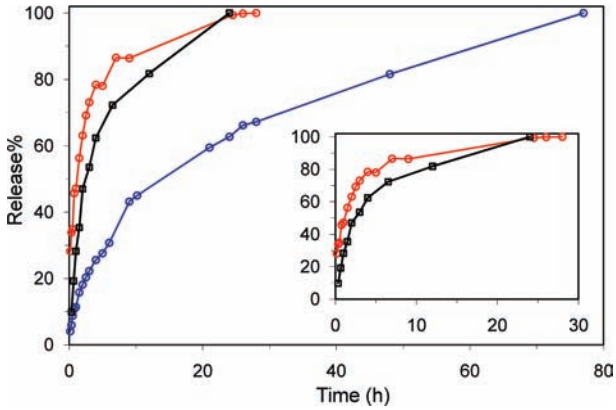

Figure 3. Release profile of the BDC-NH-BODIPY dye from the particles of **1b** in PBS buffer at 37 °C (black) as determined by fluorescence spectroscopy. Release profiles of the BDC-NH-ESCP from the particles of **1c** (red) and **1c**@silica (blue) in PBS buffer at 37 °C as determined by ICP-MS. The expanded release profiles for **1b** and **1c** are shown in the inset.

temperature range. More importantly, the BODIPY-loaded particles of **1b** and ESCP-loaded particles of **1c** were also successfully coated with silica shells using this procedure to lead to novel core−shell nanostructures denoted **1b**@silica and **1c**@silica, respectively. EDX and TGA studies indicated the coating of **1b** and **1c** particles with silica shells, while SEM and PXRD showed no change in the morphology or structure after silica coating (Figure 1f and Supporting Information). Interestingly, the release of BDC-NH-ESCP from **1c**@silica is significantly retarded with a $t_{1/2}$ of ∼14 h in PBS buffer at 37 °C, presumably due to the slow diffusion of the relatively large BDC-NH-ESCP through the silica shell (Figure 3). Consistent with this, the $t_{1/2}$ for the BDC-NH-BODIPY release from **1b**@silica was increased to ∼16 h in PBS buffer at 37 °C. The silica-coated **1b** and **1c** particles thus have adequate stabilities for biological applications.

We have evaluated the *in vitro* effectiveness of **1b**@silica as an optical contrast agent. Laser scanning confocal microscopy studies on HT-29 human colon adenocarcinoma cells showed fluorescent labeling in a dose dependent manner (Figure 4). The BODIPY fluorescence was present in cells incubated with **1b**@silica but absent in cells incubated without nanoparticles. We believe that the BDC-NH-BODIPY dye is slowly released from the **1b**@silica particles after their internalization by the cells. Control studies with the BDC-NH-BODIPY dye showed no fluorescence (Supporting Information), presumably due to its inability to cross the cell membrane. The nanosized MIL-101 (Fe) particles thus provide an efficient platform for delivering an optical contrast agent *in vitro*.

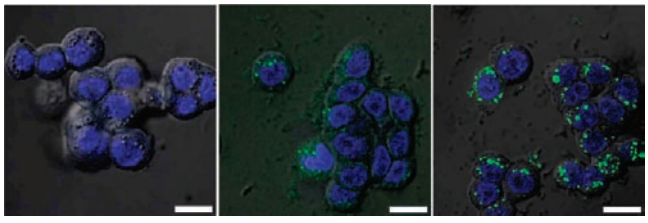

Figure 4. Overlayed DIC and confocal fluorescence images of the DRAQ5 channel (blue, nuclear stain) and the BDC-NH-BODIPY channel (green) of HT-29 cells incubated with no particles (left), 0.19 mg/mL of **1b**@silica particles (equivalent to 17 μM BODIPY) (middle), and 0.38 mg/mL of **1b**@silica particles (equivalent to 34 μM BODIPY) (right). The bars represent 25 μm.

Nanoparticles of **1c** were also evaluated to determine their anticancer efficacy on the HT-29 cell line. Treatment of HT-29 cells with nanoparticles of **1c**@silica showed appreciable cytotoxicity (IC_{50} = 29 μM); however, it was slightly less cytotoxic than cisplatin under the same conditions (IC_{50} = 20 μM). The released ESCP from **1c**@silica would presumably become active inside cells via reduction to cisplatin by endogenous biomolecules such as glutathione.[13] To increase the cytotoxicity of **1c**@silica, we functionalized the silica shell with silyl derived c(RGDfK). c(RGDfK) is a cyclic peptide known to target the $\alpha_v\beta_3$ integrin, which is overexpressed in many angiogenic tumors.[14] Cytotoxicity tests of RGD-targeted **1c**@silica gave a cytotoxicity (IC_{50} = 21 μM) similar to that of cisplatin (IC_{50} = 20 μM).

In summary, we have synthesized an iron-carboxylate NMOF of the MIL-101 structure. We have demonstrated a new strategy of delivering high payloads of imaging contrast agents and anticancer drugs by postsynthetic modifications of highly porous NMOFs. The generality of this approach should allow the design of a wide range of nanomaterials for imaging and therapeutic applications.

Acknowledgment. We thank the NIH (U54-CA119343) and NSF (DMR-0605923) for financial support and Dr. Liqing Ma for experimental help. K.M.L.T.-P. thanks the University of North Carolina for a dissertation fellowship.

Supporting Information Available: Experimental procedures, characterization data, and in vitro assays. This material is available free of charge via the Internet at http://pubs.acs.org.

References

(1) (a) Eddaoudi, M.; Kim, J.; Rosi, N.; Vodak, D.; Wachter, J.; O'Keeffe, M.; Yaghi, O. M. *Science* **2002**, *295*, 469. (b) Kitagawa, S.; Kitaura, R.; Noro, S. *Angew. Chem., Int. Ed.* **2004**, *43*, 2334–2375. (c) Evans, O. R.; Lin, W. *Acc. Chem. Res.* **2002**, *35*, 511.
(2) Li, H.; Eddaoudi, M.; O'Keeffe, M.; Yaghi, O. M. *Nature* **1999**, *402*, 276–279.
(3) Férey, G.; Mellot-Draznieks, C.; Serre, C.; Millange, F. *Acc. Chem. Res.* **2005**, *38*, 217–225.
(4) Férey, G.; Mellot-Draznieks, C.; Serre, C.; Millange, F.; Dutour, J.; Surblé, S.; Margiolaki, I. *Science* **2005**, *309*, 2040–2042.
(5) (a) Horcajada, P.; Serre, C.; Vallet-Regí, M.; Sebban, M.; Taulelle, F.; Férey, G. *Angew. Chem., Int. Ed.* **2006**, *45*, 5974–5978. (b) Horcajada, P.; Serre, C.; Maurin, G.; Ramsahye, N. A.; Balas, F.; Vallet-Regí, M.; Sebban, M.; Taulelle, F.; Férey, G. *J. Am. Chem. Soc.* **2008**, *130*, 6774–6780.
(6) (a) Lin, W.; Rieter, W. J.; Taylor, K. M. L. *Angew. Chem., Int. Ed.* **2009**, *48*, 650–658. (b) Spokoyny, A. M.; Kim, D.; Sumrein, A.; Mirkin, C. A. *Chem. Soc. Rev.* **2009**, *38*, 1218–1227.
(7) (a) Rieter, W. J.; Taylor, K. M. L.; An, H.; Lin, W.; Lin, W. *J. Am. Chem. Soc.* **2006**, *128*, 9024–9025. (b) Rieter, W. J.; Pott, K. M.; Taylor, K. M. L.; Lin, W. *J. Am. Chem. Soc.* **2008**, *130*, 11584–11585. (c) Taylor, K. M. L.; Rieter, W. J.; Lin, W. *J. Am. Chem. Soc.* **2008**, *130*, 14358–14359.
(8) For leading references in postsynthetic modifications of MOFs, see: (a) Kiang, Y.-H.; Gardner, G. B.; Lee, S.; Xu, Z.; Lobkovsky, E. B. *J. Am. Chem. Soc.* **1999**, *121*, 8204–8215. (b) Seo, J. S.; Whang, D.; Lee, H.; Jun, S. I.; Oh, J.; Jeon, Y. J.; Kim, K. *Nature* **2000**, *404*, 982–986. (c) Wu, C.-D.; Hu, A.; Zhang, L.; Lin, W. *J. Am. Chem. Soc.* **2005**, *127*, 8940–8941. (d) Wang, Z.; Cohen, S. M. *J. Am. Chem. Soc.* **2007**, *129*, 12368–12369. (e) Mulfort, K. L.; Farha, O. K.; Stern, C. L.; Sarjeant, A. A.; Hupp, J. T. *J. Am. Chem. Soc.* **2009**, *131*, 3866–3868. (f) Wang, Z.; Cohen, S. M. *Chem. Soc. Rev.* **2009**, *38*, 1315–1329.
(9) During this research, a report appeared on the synthesis of the bulk Fe MIL-101 phase with purely NH_2-BDC bridging ligands. However, our conditions only produced the Fe MIL-88B phase when 100 mol % NH_2-BDC was used. Bauer, S.; Serre, C.; Devic, T.; Horcajada, P.; Marrot, J.; Férey, G.; Stock, N. *Inorg. Chem.* **2008**, *47*, 7568–7576.
(10) Some reactions resulted in the formation of small amounts of micron sized particles, which could be easily separated from the desired nanoparticles by centrifuging at low speeds (3000 rpm).
(11) Upon decomposition of the nano-sized MIL-101 (Fe) in phosphate buffer, some of the Fe^{3+} ions form an insoluble material, likely some forms of iron phosphates, which are not released from the dialysis bag. Therefore ICP-MS analysis for Fe released from the dialysis bag does not give true stability results.
(12) (a) Rieter, W. J.; Taylor, K. M. L.; Lin, W. *J. Am. Chem. Soc.* **2007**, *129*, 9852–9853. (b) Lu, Y.; Yin, Y.; Mayers, B. T.; Xia, Y. *Nano Lett.* **2002**, *2*, 183.
(13) (a) Carr, J. L.; Tingle, M. D.; McKeage, M. J. *Cancer Chemother. Pharmacol.* **2002**, *50*, 9. (b) Feazell, R. P.; Nakayama-Ratchford, N.; Dai, H.; Lippard, S. J. *J. Am. Chem. Soc.* **2007**, *129*, 8438.
(14) Lee, J. W.; Juliano, R. L. *Mol. Biol. Cell* **2000**, *11*, 1973.

JA906198Y